第9卷 第5期
2001年10月
光学 精密工程
OPTICS AND PRECISION ENGINEERING
Vol. 9, No. 5
Oct., 2001

Article ID: 1004-924X(2001)05-0405-06

Present Status of EUV Interferometer Development at the Research Center for Soft X-ray Microscopy

Masaki Yamamoto, Tadashi Hatano, Minaji Furudate

(Research Center for Soft X-ray Microscopy, Institute of Multidisciplinary Research for Advanced Materials, Tohoku University, Japan)

Abstract: A new interferometer for extreme ultraviolet (EUV) radiation with a laser produced plasma (LPP) laboratory source is under construction. The LPP source is operated with a Sn solid rod target on which pulsed YAG laser is focused to produce high temperature plasma emitting EUV radiation. The source is equipped with a newly designed debris stopper protecting a condenser multilayer mirror from the particle debris of the target. The condenser mirror focuses the light onto an EUV beam-splitter to form transmitted and reflected paths for producing interference fringes of a sharing type. The optical configuration is of a common path based on a triangular path type with a focusing at the beam-splitter, which is enabled to produce fringes by a low coherence radiation with a standard optical quality beam-splitter. The fringes are recorded by an imaging plate with pixels as small as 25μm. The dynamic range of linearity in detection of the EUV light was found to be more than 10^4 with sensitivity of 10^4 photons/pixel, enough for the purpose of interferogram recording, possibly with one laser shot.

Key words: soft X-ray interferometers; multilayer mirrors; figure error; imaging optics
CLC number: TH744.3 **Document code:** A

1 Introduction

In the extreme ultraviolet (EUV) wavelength region, figured multilayer mirrors are now opening up new application fields of EUV imaging optics such as a telescope, a microscope, and more advanced EUV lithography camera[1-3]. Typical wavelength λ of the application is around 13nm, which is short enough to improve the resolution limited by the diffraction. The photon energy is 95eV, which is high enough to observe difference in scattering factors of atoms composing materials including biological samples.

To realize the expected resolution, we need to improve the wave-front accuracy of the optics to the required level for imaging. For a standard quality optics of $\lambda/4$, the surface finish should be within $\lambda/8$ in case of reflection optics, which is 1.6nm in terms of the figure error at the substrate surface. This requires superpolishing techniques with accurate means of figure error measurements. For further improvement towards sub-nm values needed for high quality optics, it is necessary to develop a method to measure the wave-front error of an individual mirror at the wavelength of use as well as a method to correct the measured errors.

The EUV reflection by the multilayer mirror is governed by constructive interference inheriting characteristic dependence of reflection phase and amplitude as a function of the angle of incidence and the wavelength. This actually brings a new accurate means of wave-front error correction by milling or by figuring applied at the surface of the multilayer stack[4]. In other words, the errors can be corrected to the accuracy of 0.1nm provided that the errors are measured to this accuracy. The most promising method of this high accuracy measurement should be realized by "at wavelength" measurements, with an EUV interferometer.

Received date: 2001-08-29; **revised date:** 2001-10-08

The first EUV interferometer for this purpose was developed at the beamline of ALS. It utilizes zone plate optics for imaging and gratings for splitting wave-front. The system is successfully used to measure the EUV wave-front of a multilayer mirror and also an imaging optics[5]. An interferometer of similar configuration is also developed at a beamline of NEW SUBARU, Himeji, Japan. These systems prove the importance of the at wavelength measurements. Nevertheless, these systems are insufficient for further development of EUV imaging optics due to limitations of the location and the machine time of the synchrotron radiation facilities.

To ease the limitations, we are developing a laboratory-used EUV interferometer at the Research Center for Soft X-ray Microscopy. In the next section, the configuration of the interferometer consisting of a light source, interference optics, and the detector is described. Each part will be described with technical importance involved. Particular emphasis will be put on a debris stopper since it should be useful for other applications with the laboratory EUV source.

2 Design of the EUV interferometer

The interferometer for the EUV radiation requires extremely high accuracy due to the short wavelength. As mentioned in the previous section, 0.1nm figure error should be measured by the interferometer. At the wavelength of 13nm, the phase term of $4\pi n/\lambda$ is approximately equal to 1, with the complex refractive index n of material being very close to 1. Therefore, a figure error Δd in the nm unit causes a phase shift of Δd rad.

Taking into account the sub-nm accuracy and optical characteristics of materials, the construction of the interferometer needs to overcome the following difficulties:

1. At the EUV wavelength, no transparent material exists. The interferometer should be formed basically with reflection optics. Exception would be very thin membranes of a few hundred nm or less such as free-standing filters and beamsplitters. Even air absorbs the radiation. Accordingly, the whole optical path should be kept under vacuum to avoid absorption of air.

2. The coherence of the laser produced plasma source is very poor. For the interference fringe formation, the interferometer needs to be formed by a common path configuration.

3. Optical elements inserted in the optical path should be precise enough to give negligible wave-front errors within the order of 0.1nm.

4. High precision optical stages are needed for precise alignment.

5. Vibration causing path fluctuations should be avoided during exposure for the fringe pattern recording.

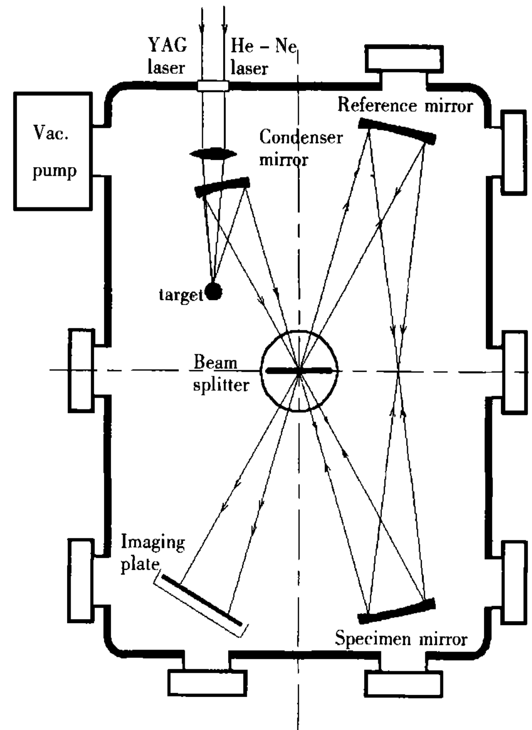

Fig. 1 Schematic plan view of the EUV interferometer

For the difficulty 1, we decided to use a vacuum chamber of 1.5m × 1.2m × 0.6m large enough to accommodate the whole optics of various kinds for development. The vacuum needed is of a few Pa or less to avoid absorption, which is easily realized by a standard vacuum technology. The difficulties 2 and 3 are related to the actual optical con-

figurations. We have sought for common path configurations with reflecting optics which can accommodate the focusing of the beam at the beam splitting point. With the focusing, the requirements for the wave-front error should be satisfied in practical way by reducing the effective area of the beam illumination.

Among the common path optical configurations satisfying these, we selected a triangle path configuration with the focusing at a beam splitter surface for versatility. Figure 1 shows the optical configuration of our system under development. It consists of a LPP source, optics, and a detector set on an optical bench of honeycomb structure. The optical bench is supported directly on a vibration isolation bench locating underneath outside of vacuum. Metal bellows are used to isolate vibration and keep the vacuum off the chamber. The vacuum chamber is supported firmly on a floor.

3 Design and operation principle of the debris stopper

It has been known that the debris particles or more specifically highly ionized ions out of high temperature plasma can be as fast as a few to a few hundreds of km/s that may damage the multilayer mirror. The particles of large volume up to a few μm in diameter are also observed though the nominal speeds should be as slow as a few tens to hundreds of m/s. These slow debris will be deposited on the multilayer mirror, thus reducing the reflectance.

To solve these debris problems, many methods have been reported[6-11]. For the interferometer application, high efficiency and easy selection of the EUV wavelength by using various solid metal targets are preferable. The slow debris of the metal targets are usually very large in size and mass and form main volume of the debris particle. Due to the large mass, it is difficult to change the course of travel by electromagnetic forces unlike the small ions. Therefore, we have decided to develop a mechanical shutter to stop these large debris.

In designing a debris stopper, we assumed a numerical aperture (NA) of 0.2 for practical applications of imaging and interferometry. For this NA, a standard spinning disc chopper is unable to be used since the opening should have a diameter in proportion to the distance from the source. A large opening has essential problem of passing slower debris periodically by every spinning interval.

The design and operation principle of our new debris stopper[12] free from the problem will be described in the next section.

3.1 New design

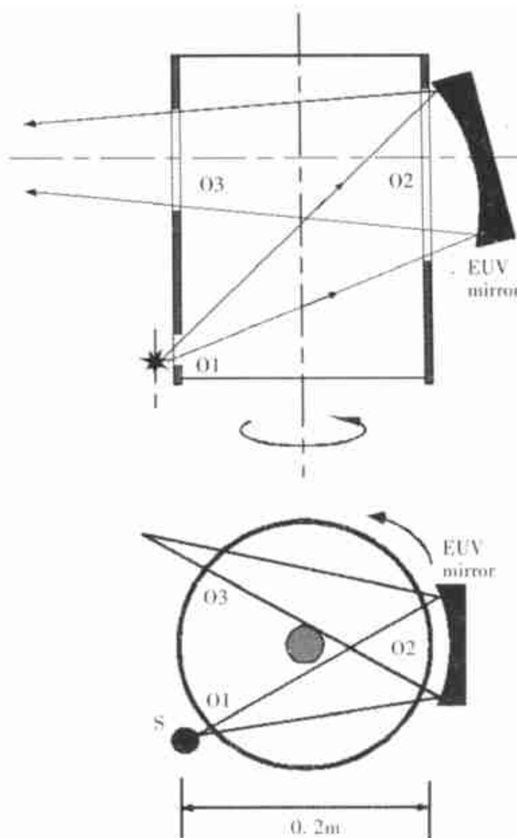

Fig.2 Schematical side view (upper) and cross sectional view (lower) of the debris stopper

Figure 2 shows a schematic side view (upper) and a cross sectional view (lower) of the debris stopper. The stopper is a hollow cylinder with its spinning axis fixed to a flange of the chamber and is suspended by magnetic bearings enabling to spin at 6000rpm under vacuum. It is 20cm in diameter and is mounted between a LPP source and a con-

denser multilayer mirror M1 of 10cm in diameter.

In addition to a small opening O1 the cylinder has 3 openings O2, O3, and O4, which are 10cm in diameter and equally spaced. At this configuration, the period of rotation is 10ms with the cylinder wall speed of 62.8m/s. The cylinder closes the light path as it spins and stops the particles emitted from the source point. As shown in the figures, the opening O1 locates at a level which differs from others and is much smaller than 7mm in diameter since it comes very close to the source S at the timing of every laser shot.

3.2 Operation principle

Figure 3 shows position vs. time diagram of debris particles traveling to the direction of the center of the mirror. The origin of the time is taken at the timing of the laser shot to produce plasma. The O1 and O2 locate 1cm and 21cm away from the source as shown in the vertical axis of this figure. The debris particles traveling to the mirror center appear as lines of different slopes representing their speed of travel. Horizontal solid bars in Fig. 3 show the walls of the cylinder with periodical appearance of the opening in time sequence. In the bar at 21cm away, O2 is appearing at 10ms at every rotation thereafter. This shows that the O2 is in the open status for approximately 1/6 of a period of one rotation, which is 1.7ms, then comes to the open status at every successive rotation. This depicts the problem of mechanical shutters described above, i.e., after the first open timing, successive appearance of opening will pass the corresponding slower debris. This difficulty has been solved in our design by the opening O1.

In the solid bar of O1 at 1cm away level, the next open status comes at 10 ms after the shot as in the case of O3, but with much shorter gap with a ratio of the open status to the close of much small 1/90. Thus, the slower debris that could pass the wall at 21cm level are stopped at 1cm away by the outside of the wall.

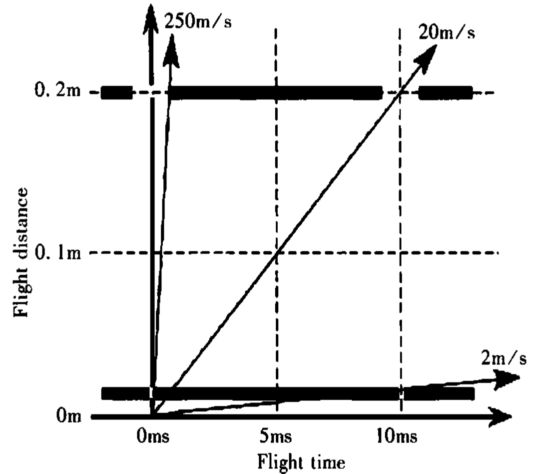

Fig. 3 Diagram of debris travel shows the stopping principle. Inclination of the lines shows the speed of the debris

Since the debris of 2m/s travels only 0.2 mm within the 0.1ms open interval of O1, the cylinder wall of 3mm is sufficiently thick to stop this slow debris as well as any slower debris arriving at O1 thereafter. Thus, all slow debris are stopped completely.

In this configuration, O2 can be set as the critical shutter to stop the highest speed particles at the farthest point from the target with a large margin. In actual design, more than three openings of 10cm in diameter can be made that allow operation of the laser at a three times or higher repetition rates than the spinning rate.

At the spinning speed of 6000rpm, the highest speed of debris stopped by O2 at the center of the mirror is 62.8/(5cm/21cm) = 264m/s. With the design described here, all particles slower than 264m/s are completely stopped under high vacuum.

Although the details are not described here, preliminary experiment was performed with a quartz crystal thickness monitor detecting the mass of arriving debris. In this experiment, the main peak of the debris speed distribution was observed at slower than 25m/s with a Sn target, suitable for the 13nm wavelength radiation. It was also found

that at a spinning speed of 6000rpm, 84% of the total mass of the debris was removed at the mirror position.

It is estimated that particles faster than this value mainly consist of monomers ionized. We are now extending experiments to trial treatments of the monomers such as an electro- magnetic force to slow down the speed and/or to deflect the course of travel.

It should be noted here that the method described here uses gas-free elements that cause increase of partial pressure of the vacuum chamber. Under a high vacuum, the debris particles will be removed as predicted by theory since no practical collision will take place resulting scattering before reaching the wall of the debris stopper.

4 Detector

For recording the interferogram, the 2- D detector needs to have high sensitivity, good linearity and a large number of pixels sufficient for recording dense interference fringe patterns. A commercially available soft X- ray CCD detector has limited number of pixels, which is insufficient for final recording though it is needed for alignment purpose as a real time monitor.

We have carried out separate experiments to find EUV characteristics of an imaging plate detector, which has been considered as the detector of hard X- ray radiation. For the experiment, a laboratory reflectometer with a LPP source[13] was used. EUV light of specific wavelength was selected by the constant deviation monochromator and delivered to the imaging plate set at the sample holder. With variation of dose by the number of shots of YAG laser, we found good linearity of more than 10^4 and also high sensitivity of 10^4 photons/mm^2. This shows that one shot of YAG laser could be intense enough to have the fringe pattern for evaluating the figure error. If this is the case, vibration would be of no problem.

5 Method of figure correction

Provided that the figure errors are measured by an EUV interferometer, correction of the errors can be done by milling of the multilayer periods as proposed in a recent publication[4]. The method enables correction with accuracy of 0. 1nm as summarized in the following.

The milling method relies upon the physical optics effects of the EUV multilayers that the reflection at each interface is very small and the large reflection is effected by constructive interference in the total volume of the multilayer structure[14]. This means that a phase correction layer prepared at the surface should work as that of a transmission one.

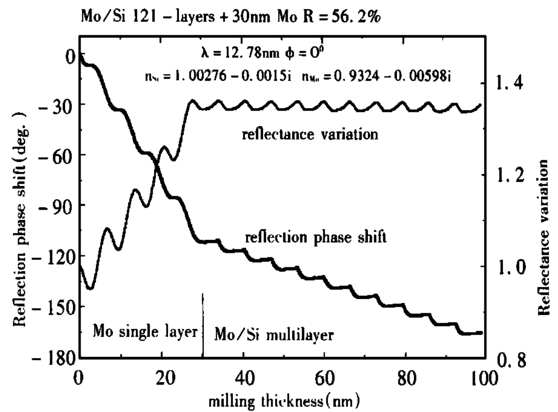

Fig. 4 Phase shift and relative reflectance calculated as a function of milling thickness from the surface of EUV multilayer mirror demonstrate sub-nm figure error correction. A 30nm thick Mo layer was added on the surface of Mo/Si 121 layers to demonstrate coarse phase correction. The reflection phase correction of 180° is equivalent to a substrate figure error correction of 3. 2nm (after Ref. [4]).

In the transmission optics, the wave-front is governed with a thickness multiplied by a refractive index difference (1- n). In the EUV region, the difference is of an order of 0. 01[15]. Consequently, the tolerance in thickness control for the wave-front error correction is increased by this factor of

several 10ths as already pointed out by Braat[16]. The optical path described as $(1-n)d$ can be controlled with great accuracy by adjusting the layer thickness d. His proposal is promising if there is a transparent material available, which is not the case in the EUV. The phase shift introduced in this way inevitably suffers from a loss in intensity of reflected waves.

With detailed theoretical study with our layer by layer calculation[14], we found that the milling of the multilayer itself hypothetically realizes the ideal transparent layer with negligible reflectance reduction, provided that the multilayer has been fabricated up to an enough number of periods where the reflectance increase is in saturation. The calculation predicted the usefulness of method, i. e., 0.1- nm accuracy phase correction by milling of the multilayer surface.

This is especially interesting when a total amount of correction needed is relatively small within ~ 90° in reflection phase, which is 1.6nm in a figure error. The milling method extends the practical technological limit of 1nm of current super polishing techniques to the required 0.1nm. In this multilayer milling, the reflectance reduction can be made as small as the order of ±0.1%.

It should be noted that the roughening of the surface by milling will cause negligible effect on reflection due to the small enough refractive index difference in the EUV.

References:

[1] Kinoshita H, Kurihara K, Ishii Y, et al. Soft-X-ray reduction lithography using multilayer mirrors[J]. J. Vac. Sci. Technol, 1989, (B7): 1648- 1651.

[2] Kinoshita H, Kurihara K, Mizota K, et al. Large- area, high resolution pattern replication by use of a two- aspherical- mirror system[J]. Appl. Opt, 1993, 32: 7079.

[3] Gwyn C W, Stulen R, Sweeney D, et al. Extreme ultraviolet lithography[J]. J. Vac. Sci. Technol, 1998, (B16): 3142.

[4] Masaki Yamamoto. Sub- nm figure error correction of an EUV multilayer mirror by its surface milling[J]. Nucl. Instrum. Methods A, 2001, 467(8): 1282- 1285.

[5] Medecki H, Tejnil E, Goldberg K, et al. A Phase- shifting point diffraction interferometer[J]. Opt. Lett, 1996, 21: 1526.

[6] Silfvast W T, Richardson M C, Bender H, et al. Laser- produced plasmas for soft X- ray projection lithography[J]. J. Vac. Sci. Technol, 1992, B10: 3126- 3133.

[7] Richardson M, Silfvast W T, Bender H A, et al. Characterization and control of laser plasma flux parameters for soft- X- ray projection lithography[J]. Appl. Opt, 1993, 32: 6901- 6910.

[8] Fiedorowicz Henryk, Bartnik andrzej, Roman Jarocki, et al. Characterization and optimization of a laser- produced X- ray source with a gas puff target[J]. SPIE, 1999, 3767: 10- 20.

[9] Hertz H M, Berglund M, Hansson B A M, et al. Liquid- target laser- plasma sources for EUV and X- ray lithography [J]. SPIE, 1999, 3736: 2- 9.

[10] Kandaka Noriaki, Kondo Hiroyuki. Effective reduction of debris emitted from a laser- produced plasma[J]. Jpn. J. Appl. Phys, 1998, 37: L174- L176.

[11] Shmaenok L A, Bijkerk F, Bruinemean C, et al. Developments of a high- power, low- contamination laser plasma source for EUV projection lithography[J]. SPIE, 1995, 2523: 113- 121.

[12] Yamamoto M, Furudate M, Sato N, et al. Compact debris shutter design of a laser- produced plasma source for high NA application[J]. SPIE, 2000, 4146: 128- 131.

[13] Nakayama Shigeru, Yanagihara Mihiro, Yamamoto Masaki, et al. Soft X- ray reflectometer with a laser produced plasma source[J]. Physica Scripta. 1990, 41: 754- 757.

[14] Yamamoto M, Namioka T. Layer- by- layer design method for soft- X- ray multilayers[J]. Appl. Opt. 1992, 31: 1622- 1630.

[15] http://www- cxro.lbl.gov/optical_constants/

[16] Braat J, KubiakG D, Kania D, et al. Proc. OSA TOPS on EUVL[A]. 1996, OSA[C], 1996, 152- 155.